Supporting Information

Substrate-Dependence of Ru Active Unit Anchored on Metal Oxides for Oxygen Evolution Reaction

Haixiang Yang[a], Jianming Gu[a], Hua Gui Yang[a], Haiyang Yuan*[a]

[a] Key Laboratory for Ultrafine Materials of Ministry of Education, Shanghai Engineering Research Center of Hierarchical Nanomaterials, School of Materials Science and Engineering, East China University of Science and Technology, Shanghai 200237, China

Note S1. Calculation of electrochemical decomposition potential (U_{dec}) of metal center

To assess the stability of metal center in metal oxides, the electrochemical decomposition potential (U_{dec}) was calculated, which can be used to determine the stability of metal center. The dissolution of metal center can be displayed as follows:

$$\text{sur-M} + x\text{H}_2\text{O} \rightarrow \text{sur-vac} + \text{MO}_x + 2x(\text{H}^+/\text{e}^-)$$

The specific electrochemical decomposition potential (U_{dec}) of metal center can be written as:

$$\Delta G_{dec} = G(\text{sur-vac}) + G(\text{MO}_x) + 2xG(\text{H}^+/\text{e}^-) - G(\text{sur-M}) - xG(\text{H}_2\text{O})$$

$$U_{dec} = -\Delta G_{dec}/ne$$

in which G(sur-M) and G(sur-vac) correspond to the energy of the perfect surface and the defective surface after M dissolves. $G(\text{H}_2\text{O})$ is the free energy of H_2O molecule (T = 298 K). $G(\text{H}^+/\text{e}^-)$ is the free energy of proton and electron (H^+/e^-), which is obtained by referencing it to the free energy of H_2 using the computational standard hydrogen electrode at U= 0 V vs. SHE (pH = 0, T = 298 K). $G(\text{MO}_x)$ is the energy of the dissolved product. The dissolved or converted compounds of different metal elements are obtained from the Pourbaix diagram of Materials Project at U = 1.5 V (vs. SHE) and pH = 0. When MO_x is solid, its energy is obtained from the total energy of its bulk. As MO_x is an ionic compound, its energy is calculated with the Pourbaix diagram in Materials Project. Taking $\text{RuO}_4\cdot\text{H}_2\text{O}_{(aq)}$ as the example, we used the Pourbaix diagram of $\text{RuO}_{2(s)}$ as the standard and calculated $G(\text{RuO}_4\cdot\text{H}_2\text{O}_{(aq)})$ by following equation:

$$\text{RuO}_4\cdot\text{H}_2\text{O}_{(aq)} + 4\text{H}^+ + 4\text{e}^- \rightarrow \text{RuO}_{2(s)} + 3\text{H}_2\text{O}$$

$$G(\text{RuO}_4\cdot\text{H}_2\text{O}_{(aq)}) = G(\text{RuO}_{2(s)}) + 3G(\text{H}_2\text{O}) - 4G(\text{H}^+/\text{e}^-) - \Delta G$$

where ΔG is the phase transition energy of $\text{RuO}_4\cdot\text{H}_2\text{O}_{(aq)} + 4\text{H}^+ + 4\text{e}^- \rightarrow \text{RuO}_{2(s)} + 3\text{H}_2\text{O}$ obtained from the Pourbaix diagram. $G(\text{RuO}_{2(s)})$ is the total energy of the bulk of RuO_2 resulting from the DFT calculation. Energies of other ionic compounds were calculated in a similar way. The dissolution/conversion products and related energies (i.e., $G(\text{MO}_x)$) in this work are listed in Table S2.

Note S2. Calculation of OER overpotential

To assess the activity of oxygen evolution reaction (OER), the general reaction mechanism of OER was considered as follows[1-3]:

$$H_2O + * \rightarrow *OH + H^+ + e^-$$
$$*OH \rightarrow *O + H^+ + e^-$$
$$*O + H_2O \rightarrow *OOH + H^+ + e^-$$
$$*OOH \rightarrow * + O_2 + H^+ + e^-$$

where * represents the active site, and *OH, *O and *OOH are the adsorbed OH, O and OOH, respectively. The OER activity is evaluated by calculating the overpotential. Firstly, we calculated the free energy of each elementary reaction in OER, and the free energies of the above four steps are written as:

$$\Delta G_1 = G_{[*OH]} - eU$$
$$\Delta G_2 = G_{[*O]} - G_{[*OH]} - e$$
$$\Delta G_3 = G_{[*OOH]} - G_{[*O]} - eU$$
$$\Delta G_4 = 4.92 - G_{[*OOH]} - eU$$

where $G_{[X]}$ (X = *OH, *O and *OOH) is the adsorption Gibbs free energy of the corresponding O-containing intermediate, which have included the zero-point energy (ΔZPE) and entropy correction ($T\Delta S$). $G_{[X]}$ were calculated relative to H_2O and H_2 at the condition of U = 0 V (vs. SHE), pH = 0 and T = 298 K. Due to the difficulty of GGA-DFT in calculating the bond energy of O_2, the experimental formation energy of two H_2O molecules (4.92 eV) was used to calculate the energy of O_2. The free energy of proton and electron (H^+/e^-) is obtained by referencing it to the free energy of H_2 using the computational standard hydrogen electrode at U = 0 V, pH = 0 and T = 298 K. The theoretical overpotential η of OER can be obtained by comparing and analyzing the steps with the largest free energy values. The calculation formula of overpotential η is as follows:

$$\eta = \mathrm{Max}[\Delta G_1, \Delta G_2, \Delta G_3, \Delta G_4,]/e - 1.23$$

With respect to the effect of the solution, we employed the implicit CANDLE solvation model by JDFTx software upon all structures, using the Garrity–Bennett–Rabe–Vanderbilt (GBRV) ultrasoft pseudopotentials (USPP).[4, 5] We corrected the solvation energy resulting from JDFTx into Gibbs free energy change (ΔG_i) of each elementary step in OER.

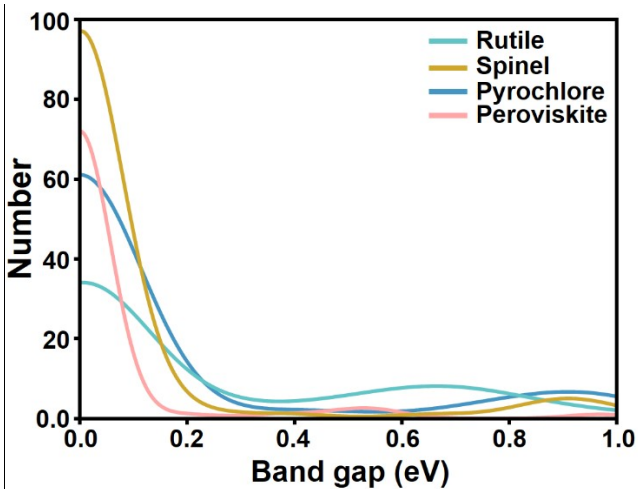

Figure S1. Numbers of rutile-, spinel-, pyrochlore- and perovskite-type metal oxides with band gaps below 1 eV.

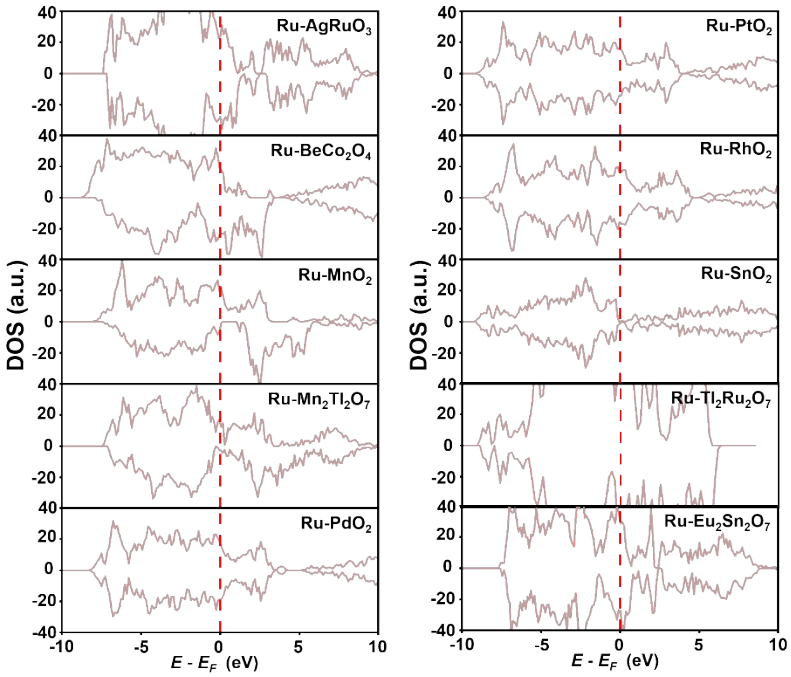

Figure S2. Total density of states (TDOS) plots of the 10 candidate materials.

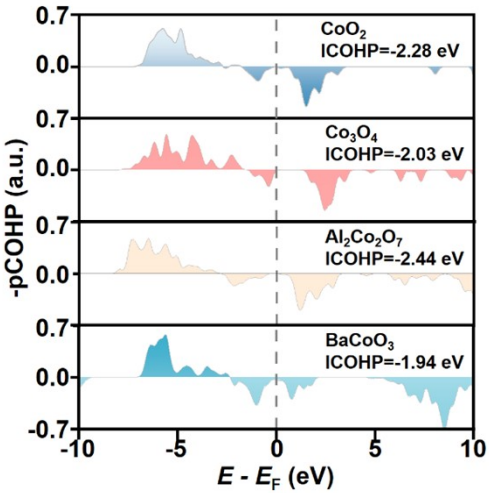

Figure S3. Projected Crystal orbital Hamilton population (pCOHP) of Co-O bonds in rutile-type CoO_2, spinel-type Co_3O_4, pyrochlore-type $Al_2Co_2O_7$ and perovskite-type $BaCoO_3$.

Table S1. Specific applied U value (U_{eff}) of 3*d* metals for DFT calculations[6].

3*d*	Cr	Mn	Cu	Fe	Sc	Zn	V	Co	Ni	Ti
U_{eff}	2.79	3.06	3.87	3.29	2.11	4.12	2.73	3.42	3.4	2.58

Table S2. Dissolution products (MO_x) and the free energy ($G(MO_x)$) of metal center at U = 1.5 V (vs. SHE) and pH = 0.

M	MO_x	$G(MO_x)$ (eV)
Cr	$HCrO_4^-{}_{(aq)}$	-40.07
Mn	$MnO_{2(s)}$	-21.43
Co	$CoO_{2(s)}$	-17.23
Ni	$Ni^{2+}{}_{(aq)}$	-3.25
Ru	$RuO_4{\cdot}H_2O_{(aq)}$	-46.32
Sc	$Sc^{3+}{}_{(aq)}$	-13.51
Ti	$TiO_{2(s)}$	-25.71
V	$VO^{4-}{}_{(aq)}$	-36.73
Fe	$Fe^{3+}{}_{(aq)}$	-5.89
Cu	$Cu^{2+}{}_{(aq)}$	-2.06
Zn	$Zn^{2+}{}_{(aq)}$	-2.65
Y	$Y^{3+}{}_{(aq)}$	-13.19
Zr	$ZrO^{2+}{}_{(aq)}$	-22.27
Nb	$Nb(OH)_{5(aq)}$	-67.99
Mo	$MoO_{3(s)}$	-33.71
Tc	$Tc_2O_{7(s)}$	-67.15
Rh	$RhO_{2(s)}$	-20.11
Pd	$PdO_{2(s)}$	-16.54
Ag	$Ag^+{}_{(aq)}$	-1.88
Hf	$Hf^{4+}{}_{(aq)}$	-15.87
W	$WO_{3(s)}$	-36.95
Li	$Li^+{}_{(aq)}$	-5.33
Na	$Na^+{}_{(aq)}$	-5.39
Mg	$Mg^{2+}{}_{(aq)}$	-8.82
K	$K^+{}_{(aq)}$	-9.86
Ca	$Ca^{2+}{}_{(aq)}$	-10.40
Rb	$Rb^+{}_{(aq)}$	-6.68
Sr	$Sr^{2+}{}_{(aq)}$	-10.12
Al	$Al^{3+}{}_{(aq)}$	-12.47
Ga	$Ga^{3+}{}_{(aq)}$	-8.49
Ge	$GeO_{2(s)}$	-19.38
In	$In^{3+}{}_{(aq)}$	-7.75
Sn	$SnO_{2(s)}$	-18.85
Sb	$Sb_2O_{5(s)}$	-41.80
Tl	$Tl_2O_{3(s)}$	-23.03
Pb	$Pb^{2+}{}_{(aq)}$	-7.64
Bi	$Bi^{3+}{}_{(aq)}$	-7.90
La	$La^{3+}{}_{(aq)}$	-17.01
Ce	$Ce(OH)^{3+}{}_{(aq)}$	-23.79
Be	$BeO_{(s)}$	-5.41
Cd	$CdO_{(s)}$	-4.76

Pr	$PrH_{2(s)}$	-19.16
Ba	$BaO_{2(s)}$	-7.30
Eu	$Eu^{3+}_{(aq)}$	-12.17
Gd	$Gd^{3+}_{(aq)}$	-23.06
Nd	$Nd^{3+}_{(aq)}$	-13.15

Table S3. 11 rutile- ,14 spinel- and 14 pyrochlore-type metal oxide candidates after the screening of electrochemical stability.

Materials	Crystal
$Mn_2Sb_2O_7$	Pyrochlore
$Mn_2Tl_2O_7$	Pyrochlore
$Tl_2Ge_2O_7$	Pyrochlore
$Tl_2Ru_2O_7$	Pyrochlore
$ZnNi_2O_4$	Spinel
$AgRuO_3$	Pyrochlore
$Bi_2Ir_2O_7$	Pyrochlore
$Bi_2Rh_2O_7$	Pyrochlore
$Bi_2Ru_2O_7$	Pyrochlore
$CuNi_2O_4$	Spinel
$FeNi_2O_4$	Spinel
$LiNi_2O_4$	Spinel
$LiFe_2O_4$	Spinel
$Eu_2Pt_2O_7$	Pyrochlore
$AlNi_2O_4$	Spinel
$Eu_2Mn_2O_7$	Pyrochlore
Co_3O_4	Spinel
$LiCo_2O_4$	Spinel
$CoNiO_4$	Spinel
Mn_2CuO_4	Spinel
$Bi_2Pt_2O_7$	Pyrochlore
$AgSbO_3$	Spinel
$LiCoO_2$	Spinel
$LiMn_2O_4$	Spinel
$BeCo_2O_4$	Spinel
$Tl_2Pt_2O_7$	Pyrochlore
$Eu_2Sn_2O_7$	Pyrochlore
$Eu_2Mo_2O_7$	Pyrochlore
$NiSb_2O_6$	Rutile
Ta_2NiO_6	Rutile
$CoSb_2O_6$	Rutile
PdO_2	Rutile

PtO_2	Rutile
MnO_2	Rutile
IrO_2	Rutile
RhO_2	Rutile
SnO_2	Rutile
$CuSb_2O_6$	Rutile
$MnSb_2O_6$	Rutile

Table S4. Average metal-oxygen (M-O) bond lengths (Å) of 1513 rutile-, spinel- and perovskite-type metal oxides.

Element	Rutile	Spinel	Perovskite
Cu	/	2.15	1.92
Mn	1.99	2.07	2.02
Ni	2.04	2.01	1.92
Pd	/	2.14	2.01
Ti	1.98	2.13	1.98
V	1.96	2.10	1.89
Mo	2.02	1.99	1.98
Ag	/	2.47	/
Ru	2.00	1.94	1.97
Sb	2.09	2.33	2.01
Al	2.14	1.99	/
Fe	1.90	2.07	1.98
Bi	2.38	2.49	2.16
Cd	2.48	2.21	/
Co	1.98	1.97	1.99
Cr	1.91	2.02	1.99
Hg	2.56	2.12	2.30
Sn	2.14	2.14	2.08
Zn	/	2.18	2.01
In	2.33	2.21	2.20
Ir	2.02	2.08	1.98
Pb	2.34	2.66	2.21
Tl	2.48	3.13	/
W	/	2.00	1.95
Ba	/	2.76	3.02
Sr	/	2.40	2.81
Dy	2.41	2.16	2.28
Pt	2.03	2.27	2.03
Ho	2.40	/	2.26
Lu	2.34	2.25	2.22
Sc	2.28	2.16	2.13
Be	/	1.69	1.60
Ce	2.35	2.44	2.29
Er	2.39	/	2.26
Eu	2.48	2.56	2.52
Gd	2.42	2.31	2.41
Ge	1.92	2.26	1.91
Hf	2.09	2.74	2.07
La	2.52	2.44	2.52
Li	/	2.14	1.99
Mg	/	2.13	2.04

Nb	2.04	2.09	2.02
Nd	2.45	2.57	2.48
Zr	2.13	2.48	2.10
Os	1.97	1.93	1.99
Pr	2.43	2.60	2.50
Re	1.95	/	1.97
Rh	2.01	2.06	2.01
Ta	1.99	2.06	2.00
Tb	2.41	2.57	2.39
Tm	2.38	/	2.24
Yb	/	/	2.21
Ga	/	1.97	1.99
Te	2.26	1.99	1.98

Table S5. Adsorption structures of *OH, *O and *OOH on Ru sites incorporated in various metal oxides. For Some metal oxides with two distinct six-coordinate metal sites that can be substituted by Ru, the substituted site was explicitly indicated in the chemical formula. For example, in Ta_2NiO_6-Ta, Ta denotes the metal site where Ru substitution occurs.

	Surface	*O	*OH	*OOH
$NiSb_2O_6$-Ni	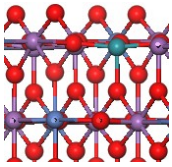	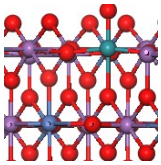	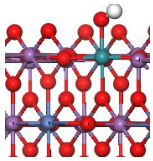	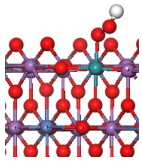
$NiSb_2O_6$-Sb	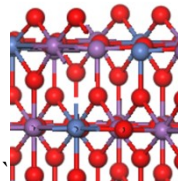	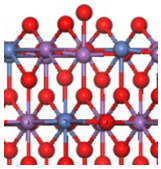	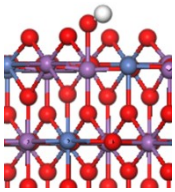	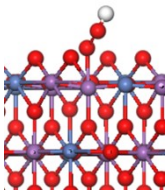
Ta_2NiO_6-Ta	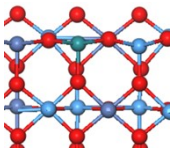	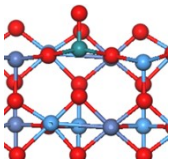	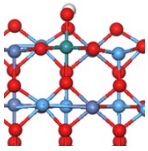	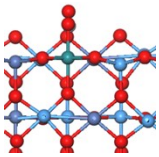
Ta_2NiO_6-Ni	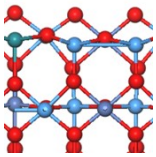	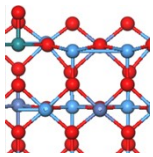	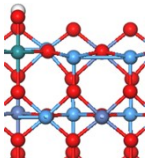	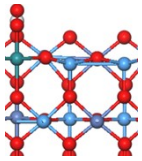
$CoSb_2O_6$-Co	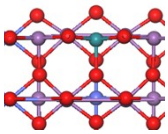	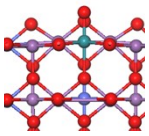	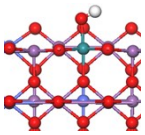	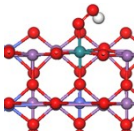
$CoSb_2O_6$-Sb	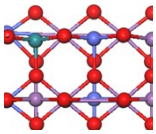	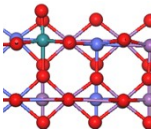	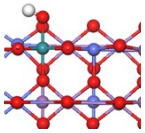	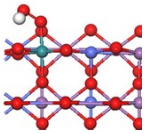
PdO_2	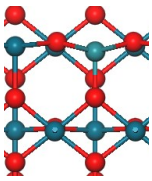	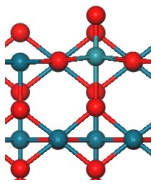	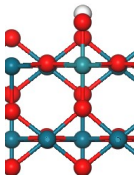	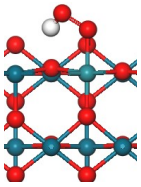
PtO_2	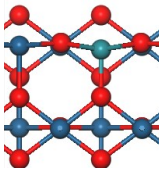	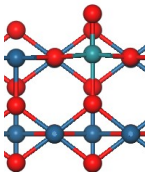	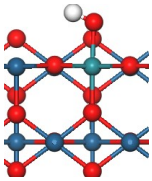	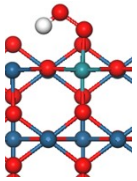

MnO_2	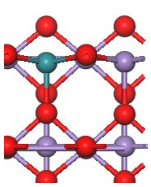	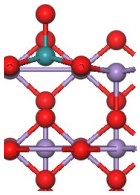	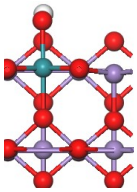	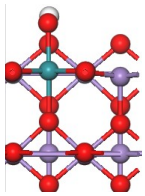
IrO_2	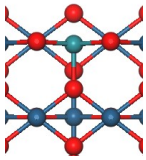	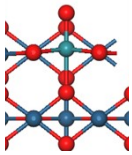	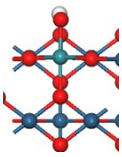	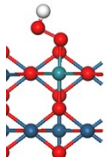
RhO_2	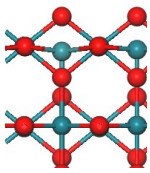	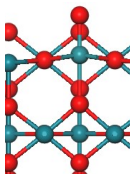	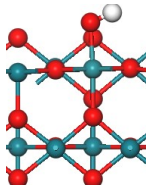	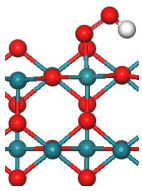
SnO_2	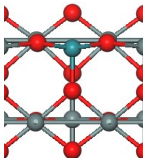	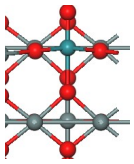	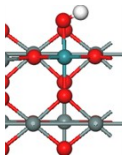	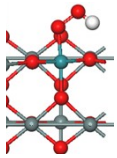
$MnSb_2O_6$-Sb	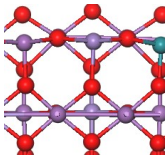	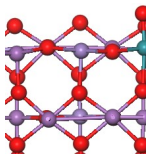	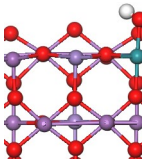	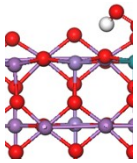
$MnSb_2O_6$-Mn	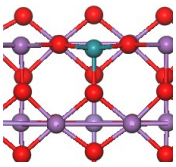	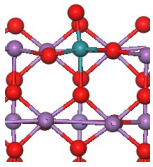	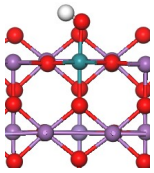	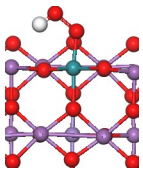
$CuSb_2O_6$-Sb	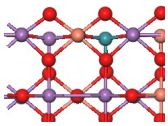	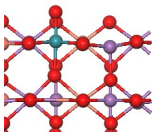	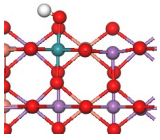	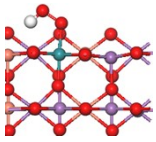
$CuSb_2O_6$-Cu	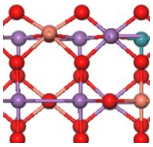	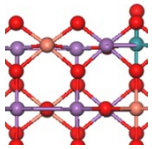	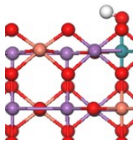	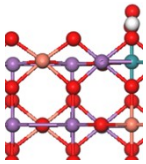
$Mn_2Sb_2O_7$	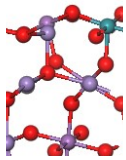	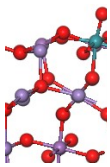	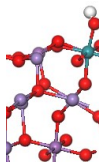	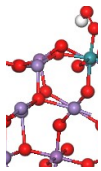
$Mn_2Tl_2O_7$	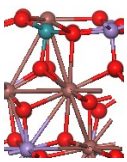	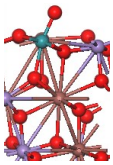	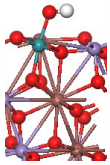	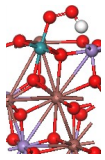

$Tl_2Ge_2O_7$	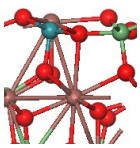	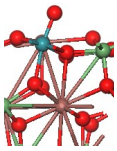	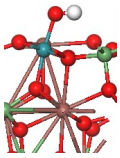	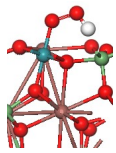
$Tl_2Ru_2O_7$	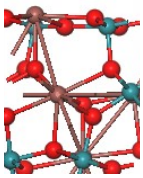	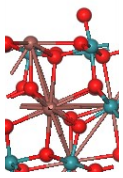	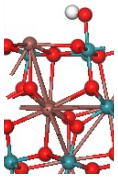	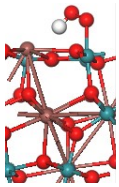
$Bi_2Ir_2O_7$	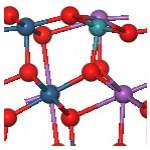	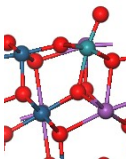	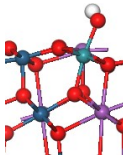	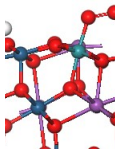
$Bi_2Rh_2O_7$	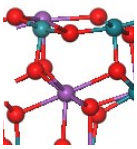	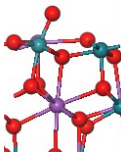	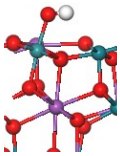	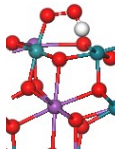
$Bi_2Ru_2O_7$	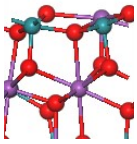	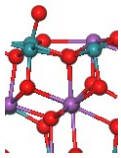	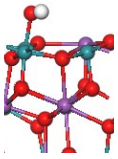	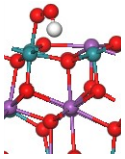
$Eu_2Pt_2O_7$	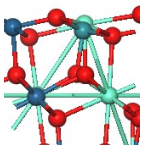	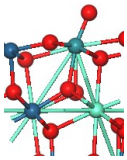	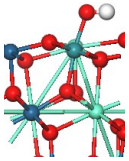	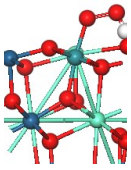
$Eu_2Mn_2O_7$	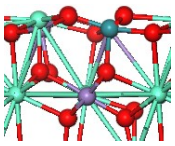	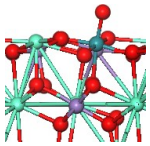	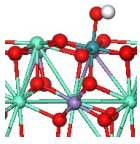	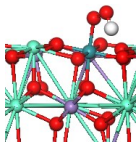
$Bi_2Pt_2O_7$	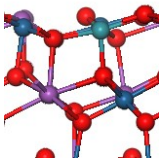		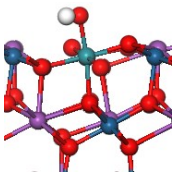	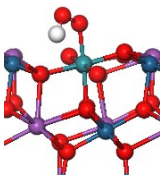
$AgRuO_3$	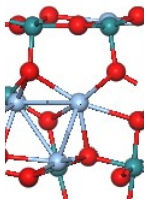	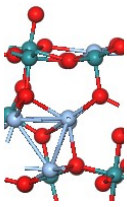	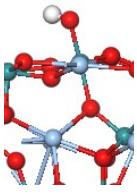	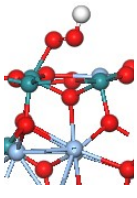
$Tl_2Pt_2O_7$	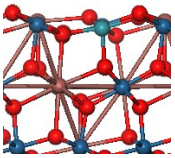	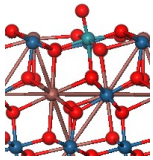	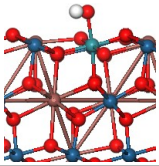	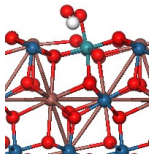

$Eu_2Sn_2O_7$	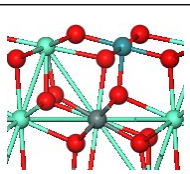	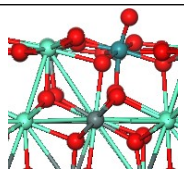	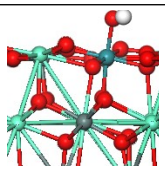	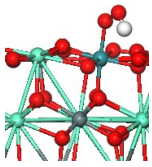
$Eu_2Mo_2O_7$	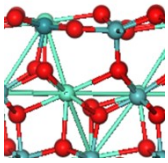	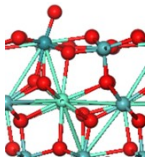	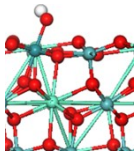	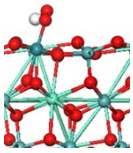
$ZnNi_2O_4$	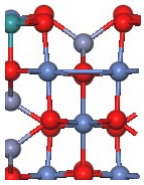	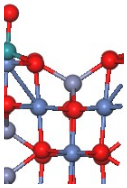	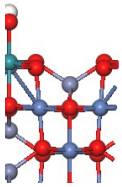	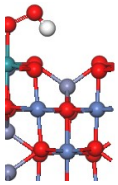
$CuNi_2O_4$	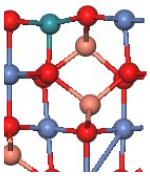	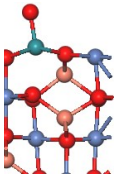	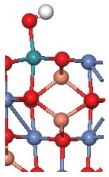	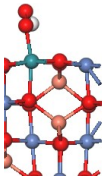
$FeNi_2O_4$	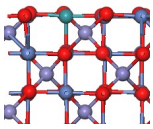	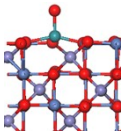	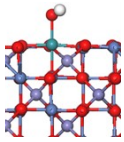	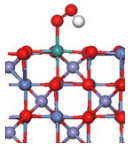
$LiNi_2O_4$	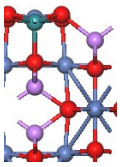	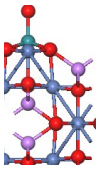	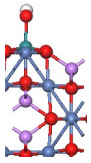	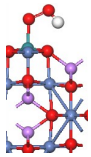
$LiFe_2O_4$	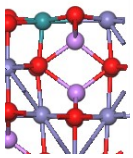	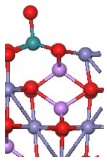	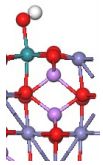	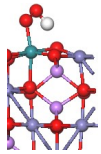
$AlNi_2O_4$	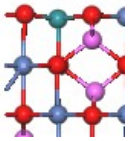	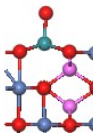	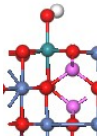	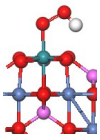
Co_3O_4	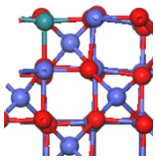	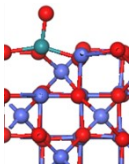	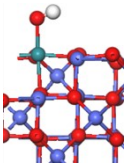	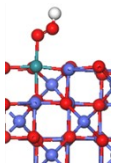
$LiCo_2O_4$	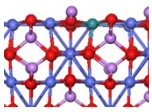	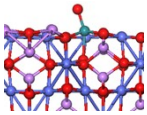	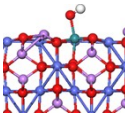	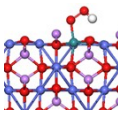

$CoNi_2O_4$	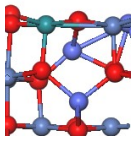	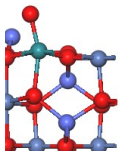	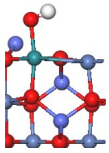	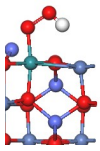
Mn_2CuO_4	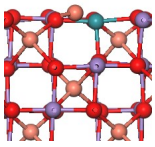	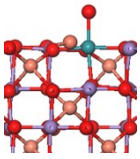	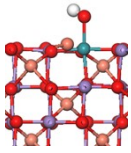	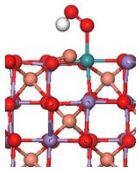
$AgSbO_3$	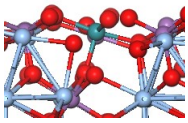	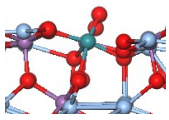	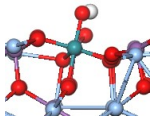	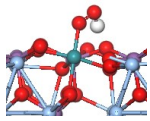
$LiMn_2O_4$	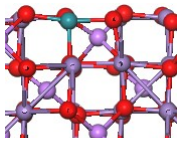	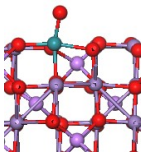	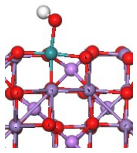	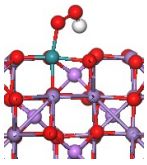
$BeCo_2O_4$	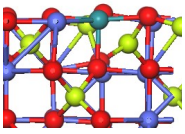	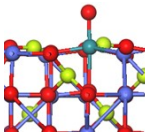	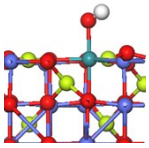	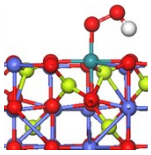
$LiCoO_2$	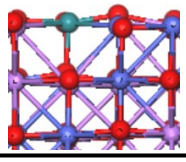	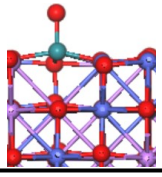	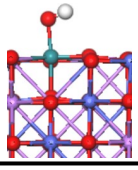	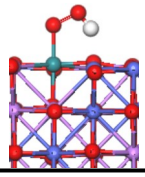

Table S6. Theoretical overpotentials of the Ru site and adjacent metal sited in the 10 potential Ru-incorporated metal oxides and the metal sites in pristine metal oxides.

Materials	Ru site	Adjacent metal site	Pristine
Ru-MnO_2	0.47	1.18	1.23
Ru-PtO_2	0.43	1.25	0.92
Ru-PdO_2	0.29	1.21	1.33
Ru-RhO_2	0.39	0.74	0.82
Ru-SnO_2	0.56	1.13	1.67
Ru-$BeCo_2O_4$	0.44	1.38	0.49
Ru-$AgRuO_3$	0.52	\	\
Ru-$Tl_2Ru_2O_7$	0.51	\	\
Ru-$Eu_2Sn_2O_7$	0.36	0.78	1.34
Ru-$Mn_2Tl_2O_7$	0.38	1.22	1.36

Reference

1. I. C. Man, H. Y. Su, F. Calle-Vallejo, H. A. Hansen, J. I. Martínez, N. G. Inoglu, J. Kitchin, T. F. Jaramillo and J. K. Nørskov, Jan Rossmeisl, *ChemCatChem*, 2011, **3**, 1159.
2. J. K. Nørskov, J. Rossmeisl, A. Logadottir, L. Lindqvist, J. R. Kitchin, T. Bligaard, H. Jónsson, *J. Phys. Chem. B*, 2004, **108**, 17886.
3. J. Rossmeisl, Z. W. Qu, H. Zhu, G. J. Kroes and J. K. Nørskov, *J. Electroanal. Chem.* 2007, **607**, 83.
4. R. Sundararaman and W. A. Goddard, 3rd, *J Chem. Phys.*, 2015, 142, 064107.
5. R. Sundararaman, K. Letchworth-Weaver, K. A. Schwarz, D. Gunceler, Y. Ozhabes and T. A. Arias, *Softwarex,* 2017, 6, 278-284.
6. I. V. Solovyev, P. H. Dederichs and V. I. Anisimov, *Phys. Rev. B*, 1994, **50**, 16861